Pharmacokinetic Modeling of Intrathecally Administered Recombinant Human Arylsulfatase A (TAK-611) in Children With Metachromatic Leukodystrophy

Steven Troy[1,2,*], Margaret Wasilewski[1,3], Jack Beusmans[4] and C.J. Godfrey[4]

Metachromatic leukodystrophy (MLD) is a lysosomal storage disease caused by deficient arylsulfatase A (ASA) activity, which leads to neuronal sulfatide accumulation and motor and cognitive deterioration. Intrathecal delivery of a recombinant human ASA (TAK-611, formerly SHP611) is under development as a potential therapy for MLD. We used serum and cerebrospinal fluid (CSF) TAK-611 concentrations measured during the phase I/II trial of intrathecal TAK-611 to develop a pharmacokinetic (PK) model describing drug disposition. CSF data were well characterized by a two-compartment model in the central nervous system (CNS); a single central compartment described the serum data. Estimated parameters suggested rapid distribution of TAK-611 from CSF into the putative brain tissue compartment, with persistence in the brain between doses (median distributive and terminal half-lives in the CNS: 1.02 and 477 hours, respectively). This model provides a valuable basis for understanding the PK distribution of TAK-611 and for PK/pharmacodynamic analyses of functional outcomes.

Study Highlights

WHAT IS THE CURRENT KNOWLEDGE ON THE TOPIC?

☑ Intrathecal delivery of recombinant human arylsulfatase A (TAK-611) is currently under investigation as a potential therapy for metachromatic leukodystrophy. The pharmacokinetic (PK) profile of intrathecal TAK-611 has not yet been reported.

WHAT QUESTION DID THIS STUDY ADDRESS?

☑ This analysis aimed to characterize the effect of different dosing regimens on the disposition of intrathecally administered TAK-611, to predict the extent to which the drug may reach and persist in the central nervous system (CNS), and to simulate the predicted PK profile of new dosing regimens.

WHAT DOES THIS STUDY ADD TO OUR KNOWLEDGE?

☑ This model provides the first PK characterization of intrathecal TAK-611. It suggests that the drug is distributed rapidly from the cerebrospinal fluid into a putative CNS compartment, where it persists between doses.

HOW MIGHT THIS CHANGE CLINICAL PHARMACOLOGY OR TRANSLATIONAL SCIENCE?

☑ The model will be used as the basis for exposure–response analyses to evaluate and predict relevant clinical outcomes in patients receiving intrathecal TAK-611. In addition, these findings may inform PK analyses of other therapeutic enzymes for intrathecal administration.

Metachromatic leukodystrophy (MLD; OMIM 250100) is a rare, autosomal recessive lysosomal storage disease (LSD) caused by deficient activity of arylsulfatase A (ASA).[1,2] MLD is commonly classified into three clinical subtypes depending on the age of the patient at symptom onset: late-infantile, juvenile, or adult.[3] The late-infantile form is generally associated with the most rapid and severe decline in motor function, whereas patients with the juvenile and adult forms tend to experience slower disease progression with changes in motor function, cognitive function, and behavior.[1,4–6] Ultimately, patients develop profound disability and die prematurely, usually owing to complications of the disease.[1,2]

There is currently no disease-specific therapy for MLD, and treatment is typically symptomatic.[3,7] Hematopoietic stem cell transplantation has been used in some patients and may delay disease progression in some individuals with juvenile or adult MLD when performed at an early stage.[3,8,9] However, this procedure carries several risks, has variable outcomes, and has shown little benefit in patients with late-infantile MLD.[3,8,9] Therefore, there remains a clear need to develop new treatments for the disease.

Enzyme replacement therapy (ERT) has been used successfully to treat somatic symptoms in patients with other LSDs.[10] However, intravenously delivered enzymes are not expected to

[1]Shire (a member of the Takeda group of companies), Lexington, Massachusetts, USA; [2]Radius Health, Waltham, Massachusetts, USA; [3]ID Remedies LLC, Medford, Massachusetts, USA; [4]Metrum Research Group, Tariffville, Connecticut, USA. *Correspondence: Steven Troy (stroy@radiuspharm.com)

Received July 19, 2019; accepted December 4, 2019. doi:10.1002/cpt.1752

cross the blood–brain barrier in therapeutic quantities, and, therefore, cannot alleviate the neurological manifestations of MLD or other LSDs.[7,11] As an alternative to intravenous ERT, intrathecally delivered ERT for LSDs has been investigated in both animal and human studies.[12–15]

In a mouse model of MLD, intrathecal (IT) administration of a recombinant human ASA (TAK-611, formerly SHP611; Shire, Lexington, MA, a Takeda company) was associated with a reduction in the lysosomal marker LAMP-1 in the white and gray matter of the brain, suggesting that TAK-611 may have therapeutic activity *in vivo*.[15] Further to this, a phase I/II clinical trial (NCT01510028) of IT TAK-611 administered via an IT drug delivery device (IDDD) in subjects with MLD has now been completed, and the drug was found to be generally well tolerated, with no drug-related or intrathecal device-related deaths or discontinuations.[16] In addition, a mean decrease in cerebrospinal fluid (CSF) sulfatide levels was observed in individuals receiving the two higher doses, 30 and 100 mg every other week (EOW), and the decline in gross motor function was less pronounced in some subjects receiving 100 mg EOW (the highest dose).[16] Subjects who completed the phase I/II study could choose to continue receiving TAK-611 at the highest dose tested (100 mg) in an extension study, which is ongoing (NCT01887938).

To evaluate and predict the potential efficacy of ERT with IT TAK-611 more effectively in patients with MLD, there is a need to understand the physiological distribution of the drug and variables that may affect this. Here, we describe the development of a population pharmacokinetic (PK) model based on serum and CSF TAK-611 concentrations measured during the phase I/II trial of TAK-611. This model characterizes the disposition of TAK-611 following IT administration in patients with MLD.

METHODS

Subjects and trial design

The phase I/II clinical trial of TAK-611 (NCT01510028) was a multicenter, open-label, dose-escalation study carried out in accordance with The Declaration of Helsinki and Good Clinical Practice guidelines. The protocol and informed consent documents were reviewed and approved by the institutional review board and/or independent ethics committee at each site participating in the study. Written informed consent was obtained from the parent(s) or legally authorized representative(s) of each patient before enrollment.

In total, 34 subjects were screened; 24 were enrolled across four dose cohorts ($n = 6$ per cohort). Individuals in cohorts 1, 2, and 3 received TAK-611 10, 30, and 100 mg (process A), respectively; those in cohort 4 received TAK-611 100 mg produced using a revised manufacturing process, which increases the levels of mannose-6-phosphate and sialic acid (process B; described in Wright *et al.*).[15] A placebo control cohort was not included owing to the unacceptable risk/benefit ratio associated with IT delivery of an inactive comparator. Participants in all cohorts had to meet the following eligibility criteria: confirmed MLD diagnosis (by deficient enzyme activity with an ASA-deficiency assay in leukocytes and an elevated sulfatide concentration in urine); first appearance of MLD symptoms at or before 30 months of age; ambulatory (able to walk 10 steps with one hand held) at the time of screening; and neurological signs of MLD at screening. In addition, subjects in cohorts 1–3 had to be younger than 12 years of age at screening, whereas those in cohort 4 had to be younger than 8 years of age at screening, with a Gross Motor Function Measure-88 (GMFM-88)[17] total score ≥ 40 at the time of screening and ≥ 35 at baseline.

An IDDD was surgically implanted in each patient after enrollment. All subjects received TAK-611 via the IDDD EOW for 38 weeks, with the end of study (EOS) defined as week 40, such that up to 20 doses were received in total. If the use of the IDDD was precluded on a scheduled dosing day, TAK-611 was administered by lumbar puncture. TAK-611 was produced by Shire (Lexington, MA; a Takeda company) using a genetically engineered human cell line via the original or revised manufacturing process,[15] and was formulated at 30 mg/mL recombinant human ASA in an aqueous isotonic solution containing 154 mM sodium chloride and 0.005% polysorbate 20 at pH 6.0. Twelve subjects missed one or more doses of TAK-611 (six subjects missed one dose, five subjects missed two doses, and one subject missed three doses). All subjects who completed the study were eligible to continue to receive TAK-611 as part of an extension study, which is ongoing (NCT01887938).

Sampling and analytical methods

Serum samples used for measurement of TAK-611 concentrations were collected at the time of the first dose (week 0) and the last dose (week 38). Samples were collected 1 hour before injection and then at 0.5, 1, 2, 4, 8, 12, 24, and 48 hours after completion of the injection. TAK-611 concentrations in CSF were measured in single samples collected before injection at baseline and initially every 2 weeks thereafter, with the frequency reduced to every 4 weeks via protocol amendment, until EOS. The presence of antidrug antibodies (ADAs) was determined in serum and CSF samples collected at baseline and every 4 weeks thereafter until EOS. Serum and CSF samples could not be obtained for all subjects at all planned time points; the model was developed based on all available measurements.

All TAK-611 and ADA assays were performed by Covance Laboratories (Chantilly, VA). TAK-611 concentrations in serum and CSF were measured using validated enzyme-linked immunosorbent assay methods, which had a detection range of 19.5–1,250 ng/mL. The presence of ADAs was determined in serum and CSF using an electrochemiluminescence bridging immunoassay (Meso Scale Diagnostics LLC, Rockville, MD) that utilized biotinylated and sulfo-tagged TAK-611 for capture and detection, respectively. ADA-positive samples were subsequently assessed for titer and neutralizing activity using an arylsulfatase A activity assay with 4-nitrocatechol sulfate as the substrate.

PK modeling

To be included in the PK analysis, subjects needed to have received at least one dose of TAK-611 and to have had at least one CSF or serum TAK-611 concentration measurement recorded. Dosing, covariate, ADA, and TAK-611 concentration data from the study were merged, formatted for analysis, and saved as comma-delimited text files in version 3.2 or above of R (R Foundation; https://www.r-project.org). Although predose TAK-611 concentrations in the CSF were generally recorded 14 days after the previous dose in line with the EOW regimen, some subjects missed one or more TAK-611 doses or CSF sampling events. On occasions when doses were missed, subsequent predose TAK-611 concentrations in the CSF used in model development were, therefore, recorded > 14 days after the previous dose. TAK-611 concentrations reported as being below the limit of quantification (BLOQ) were flagged in the dataset and excluded from the analysis, as attempts to treat the missing data as censored using likelihood-based methods[18] were unsuccessful. Covariate data were excluded from the analysis if > 10% of the values were missing; otherwise, missing values were imputed using a single imputation method based on the available data. Missing ADA values were filled in using linear interpolation between the measured values.

R was used to assemble datasets and to produce plots and summaries of the data; population PK analyses were performed using nonlinear mixed effects modeling software (NONMEM, version 7.3; ICON

Development Solutions, Ellicott City, MD). TAK-611 concentrations in CSF and serum were modeled simultaneously with differential equations using the Predictions for Population Pharmacokinetics subroutine ADVAN13, designed for solving mixed systems of stiff and nonstiff nonlinear differential equations. The first-order conditional estimation with interaction estimation method was used to estimate fixed effects (θs) and random effects (interindividual variability: ηs; residual variability: Ɛ); the distribution of interindividual random effects was assumed to be log-normal with variance–covariance matrix Ω. Concentrations were log-transformed before analysis and an additive residual error model on the log-scale was used.

During model elaboration, assessment of the model and decisions to increase complexity were based on goodness-of-fit criteria, including the following: visual inspection of diagnostic scatter plots (e.g., observed vs. predicted concentrations); successful convergence of the minimization routine with at least three significant digits in parameter estimates; plausibility of parameter estimates; precision of parameter estimates; and correlation between model parameter estimation errors (e.g., correlation between ηCL and $\eta V_{central}$) < 0.95. All parameter estimates were reported with a measure of estimation uncertainty using the standard error of the estimates (obtained from the NONMEM $COVARIANCE step). Age and weight were the main covariates included in the PK modeling; the ADA covariates (titer and neutralizing activity) were evaluated graphically. The model was used to estimate subject-specific PK parameters, which were reported and summarized. Confidence intervals (CIs) for parameter estimates were calculated via a bootstrap procedure.

The allometric model used to evaluate weight-based scaling was described by the following equations:

$$\mathrm{TV\_}V_{\mathrm{central}} = \theta_{V\mathrm{central}} \cdot \left(\frac{\mathrm{WT}}{15\mathrm{kg}}\right)$$

$$\mathrm{TV\_CL} = \theta_{\mathrm{CL}} \cdot \left(\frac{\mathrm{WT}}{15\mathrm{kg}}\right)^{0.75}$$

(TV = typical value of model parameter; WT = individual body weight; θ = estimated parameter describing typical PK parameter value for an individual of reference weight).

The final model and parameter estimates were evaluated using a visual predictive check method, which is similar to a posterior predictive check[19] but assumes that parameter uncertainty is negligible relative to interindividual and residual variance. Any problems evident in simulations were investigated and the model was developed further as necessary.

RESULTS

Population pharmacokinetic modeling of TAK-611

A PK model was developed based on data from 24 subjects with MLD who were enrolled in the phase I/II clinical trial of IT TAK-611[16] (**Figure 1**; full study design details provided in Methods). At baseline, subjects had a median (range) age of 36.5 (19.0–107) months and a median baseline weight of 14.1 (10.5–24.8) kg. The data used for model development comprised TAK-611 trough concentrations in the CSF measured every 2 or 4 weeks (**Figure 2a**) and moderately sampled concentration profiles of TAK-611 in serum over the course of 2 days, measured at both week 0 (first IT dose) and week 38 (**Figure 2b**). In total, there were 321 CSF samples (median 11 per subject; range 5–19) and 387 serum samples (median 11.5 per subject; range 1–17) available for analysis. Of these, 60 CSF samples (18.7%) and 117 serum samples (30.2%) were BLOQ. Observed CSF

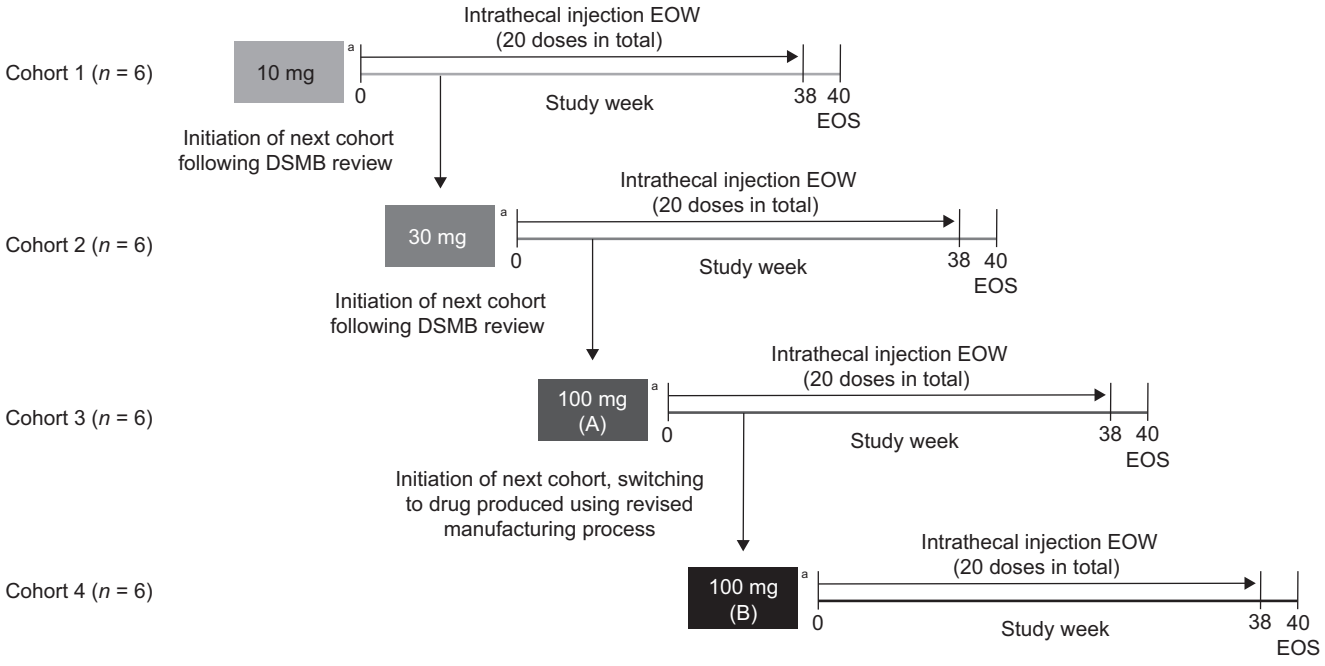

Figure 1 Design of phase I/II clinical trial of intrathecal TAK-611. Illustrated timing of sequential cohort treatment initiation is not drawn to scale. Subjects in cohorts 1–3 received TAK-611 manufactured using process A (A); cohort 4 received TAK-611 manufactured using a revised process, process B (B). Delivery of the first dose to the first subject in cohorts 2 and 3 took place ~ 1 month after the final subject in the previous cohort had received their first dose; delivery of the first dose to the first subject in cohort 4 was ~ 15 months after the final subject in cohort 3 had received their first dose. [a]An intrathecal drug delivery device was surgically implanted before treatment. DSMB, Data Safety Monitoring Board; EOS, end of study; EOW, every other week.

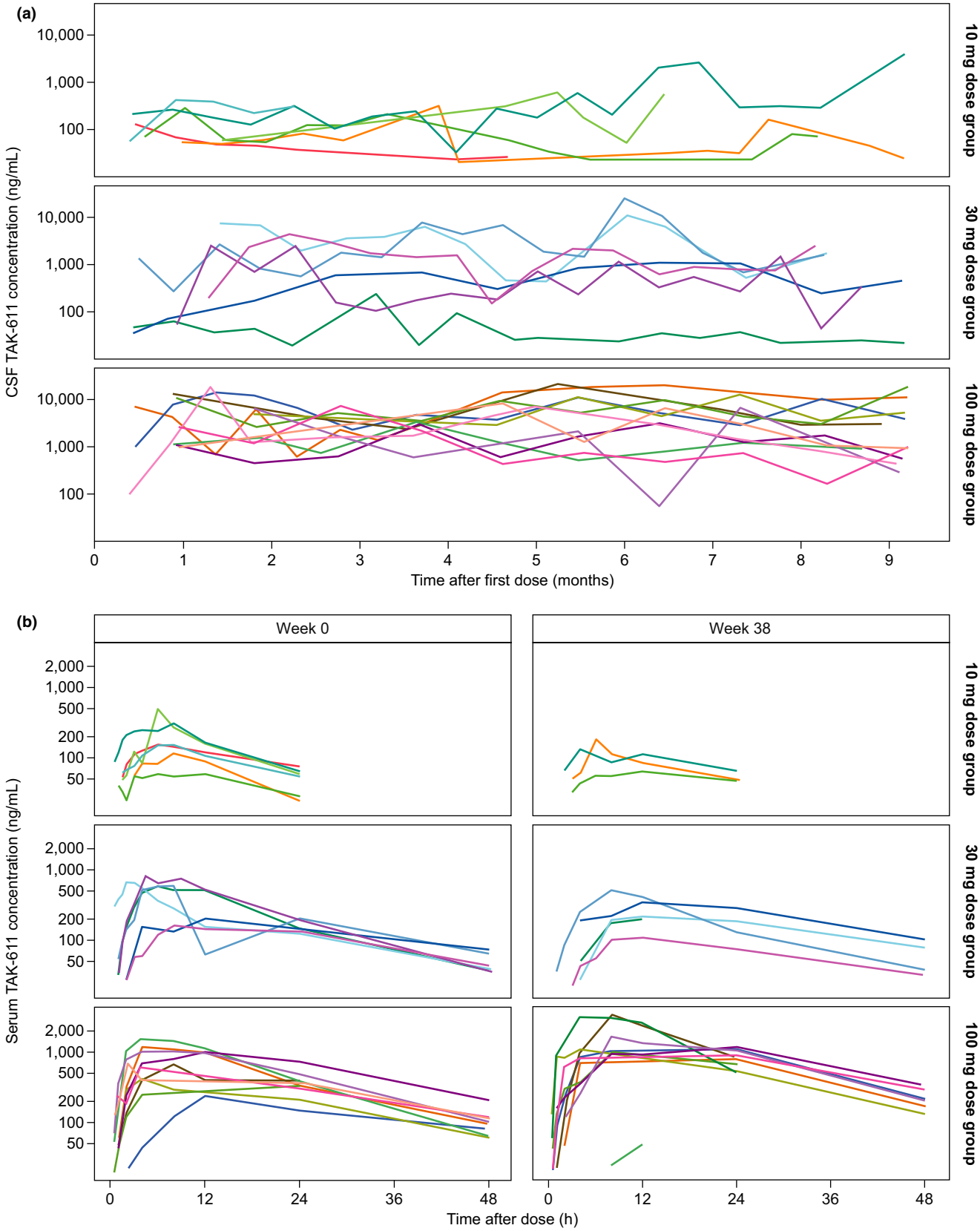

Figure 2 TAK-611 concentrations over time in (**a**) CSF (predose values)[a] and (**b**) serum (48-hour profile). [a]CSF samples for measurement of TAK-611 concentration were taken immediately before dosing and, therefore, reflect trough concentrations. CSF, cerebrospinal fluid.

trough concentrations varied considerably, both between dose groups and between individuals receiving the same dose; overall, higher doses showed a trend toward being associated with higher CSF trough concentrations.

Initial model development was based on a single CSF compartment connected via a transit compartment to a single central serum compartment. However, this starting model was unable to accommodate the observed CSF concentration data. The inclusion of a compartment peripheral to CSF, potentially representing the central nervous system (CNS) brain tissue, greatly improved the prediction of CSF data without adversely affecting the prediction of serum data. Model fit (as assessed by the Bayesian information criterion) was further improved by replacing weight-based allometric scaling of the CSF and CNS volumes with an age-based scaling method, which incorporated data on volumetric changes in CSF and white and gray matter in children aged 1–120 months.[20]

In the final model, disposition of TAK-611 after IT delivery was represented by a two-compartment model in the CNS with volumes of distribution V_{CNS} and V_{CSF} (proportional to age-based physiological volumes) and intercompartmental clearance, Q_{CSF} (**Figure 3**; **Table 1**). A hypothetical transit compartment was included to account for the exit of TAK-611 from the CSF and its delayed appearance in serum, and the transit rate was estimated with a first-order rate constant, K_{trans}. Following the appearance of TAK-611 in serum, one-compartment PKs were observed, with drug clearance and volume of distribution, $V_{central}$.

Estimated model parameters are listed in **Table 1**, and the estimated individual-level PK parameters are given in **Table 2**. The model suggested rapid distribution of TAK-611 into brain tissue, with a median (range) distributive half-life of 1.02 (0.394–1.66) hours into the CNS compartment (**Table 2**). Similarly, the median transit half-life of 1.19 (0.555–2.09) hours from CSF to serum (**Table 2**) indicated rapid distribution into the systemic circulation, with complete exit of TAK-611 from the CSF expected within ~ 6 hours. In contrast, TAK-611 had a much longer median terminal half-life in the CNS, of 477 hours (256–1,010 hours), indicating a slow release from the brain tissue back to the CSF (**Table 2**).

Covariate analysis

In addition to subject age, which was included in the model as described above, several other covariates were analyzed to determine their potential influence on the PK model. One of these was the drug-manufacturing process: subjects in cohorts 1–3 received TAK-611 manufactured using the original process (process A), whereas those in cohort 4 received TAK-611 manufactured using a revised process (process B; described in Wright *et al.*).[15] The estimated bioavailability of TAK-611 produced using process B (0.948; 95% CI: 0.546, 1.350) was not significantly different from that of TAK-611 produced using process A (reference value of 1).

Subject weight was also considered as a potential covariate for the systemic components of the model (clearance and $V_{central}$). Baseline weight was used in initial model development, but it was considered that accounting for changes in the weight of subjects throughout the study might improve model performance. Continuous weight was calculated using linear interpolation between quarterly weight measurements; however, as may be expected given the relatively short study time and limited changes in body weight, inclusion of this variable in the model did not improve the fit of the data (objective function value increased by 3.649).

The influence of ADA titer and the presence of neutralizing ADAs were assessed graphically (**Figure S1**). In serum, at week 38, five subjects had ADA titers > 1,000 (**Figure S1b**). Four of the five subjects with titers > 1,000 (two in the 10 mg dose group, one in the 30 mg dose group, and one in the 100 mg (process B) dose group) presented evidence of reduced TAK-611 concentrations in serum at week 38 (**Figure S1b**). Neutralizing ADAs were detected in three of these four subjects, all of whom had TAK-611 concentrations in serum that were BLOQ (**Figure S1b**). In CSF, observed ADA titers were lower than those in serum and, with the exception of 1 subject in the 10 mg dose group, did not have a clear effect on TAK-611 concentrations (**Figure S1a**). No neutralizing ADAs were detected in CSF.

Model performance

Goodness-of-fit plots constructed to compare observed and predicted TAK-611 concentrations indicated that the data were generally well characterized by the PK model for both CSF and

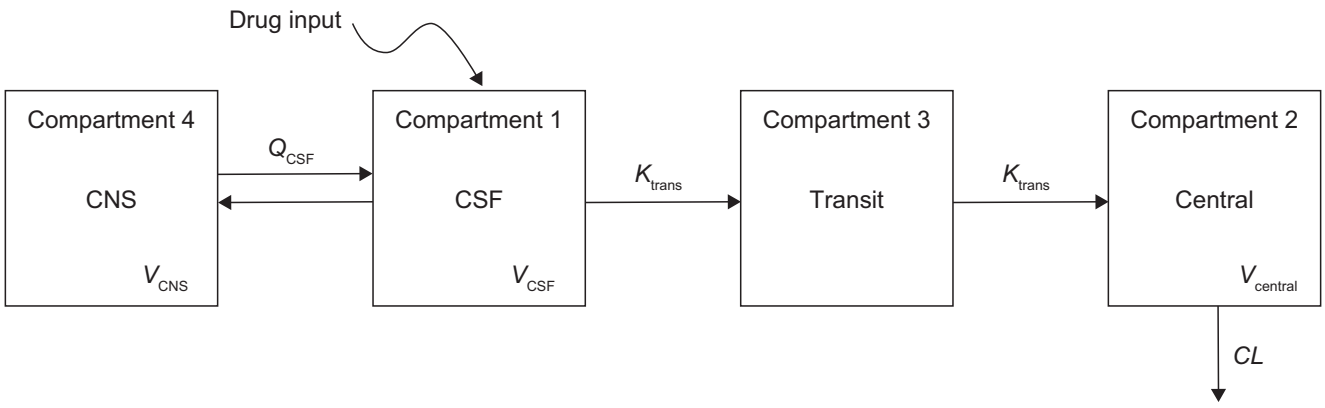

Figure 3 Final TAK-611 pharmacokinetic model. *CL*, clearance; CNS, central nervous system; CSF, cerebrospinal fluid; K_{trans}, transit rate constant; Q_{CSF}, intercompartmental clearance; $V_{central}$, volume central; V_{CNS}, volume of distribution in CNS; V_{CSF}, volume of distribution in CSF.

Table 1 Model parameter estimates

Parameter	Variable	Estimate	RSE (%)	95% CI[a]	CV	Shrinkage (%)
Fixed effects						
Proportionality of V_{CSF} to CSF volume	θ_1	0.183	76.1	(0.0889, 1.72)	–	–
Proportionality of V_{CNS} to white matter + gray matter volume	θ_2	1.69	121	(0.421, 3.97)	–	–
Intercompartmental clearance$_{CNS}$ (Q_{CNS}), L/hour	θ_3	0.00280	22.3	(0.000949, 0.0222)	–	–
Transit rate constant (K_{trans}), hour^{-1}	θ_4	0.581	40.2	(0.0917, 0.809)	–	–
Clearance$_{systemic}$, L/hour	θ_5	3.01	19.3	(2.10, 3.40)	–	–
$V_{central}$, L	θ_6	69.1	5.55	(0.963, 81.0)	–	–
Interindividual variability random effects						
Intercompartmental clearance$_{CNS}$ (Q_{CNS})	$\omega_{1,1}$	0.0607	1440	(0, 0.954)	24.6%	78.4
Transit rate constant (K_{trans})	$\omega_{2,2}$	0.176	103	(0, 0.541)	42.0%	18.7
Clearance$_{systemic}$	$\omega_{3,3}$	1.05e–08	6.30e+08	(0, 0.0753)	0.0102%	100
$V_{central}$	$\omega_{4,4}$	0.162	106	(0, 3.81)	40.3%	22.3
Distribution volume$_{CSF}$ (V_{CSF})	$\omega_{5,5}$	0.409	64.4	(0.0964, 1.24)	63.9%	11.6
Distribution volume$_{CNS}$ (V_{CNS})	$\omega_{6,6}$	0.425	341	(0, 1.11)	65.2%	56.7
Residual variability random effects						
CSF residual error (log scale)	$\sigma_{1,1}$	0.963	11.5	(0.801, 1.16)	0.981[b]	5.14
Serum residual error (log scale)	$\sigma_{2,2}$	0.456	6.09	(0.201, 0.470)	0.675[b]	5.01

CI, confidence interval; CNS, central nervous system; CSF, cerebrospinal fluid; CV, coefficient of variation; RSE, relative standard error; V_{CSF}, volume of distribution in CSF; V_{CNS}, volume of distribution in CNS.
[a]Calculated using a bootstrap procedure. [b]Reported as SD.

Table 2 Summary statistics of individual-level parameter estimates

Parameter	Mean (SD)	Median (range)
Half-life$_{CSF\rightarrow serum}$, hours	1.28 (0.421)	1.19 (0.555–2.09)
Transit rate constant (K_{trans})$_{CSF\rightarrow serum}$, hour^{-1}	0.607 (0.220)	0.581 (0.332–1.25)
Intercompartmental clearance (Q_{CNS}), L/hour	0.00279 (0.000150)	0.00277 (0.00246–0.00320)
Distributive half-life$_{CNS}$, hours	1.06 (0.326)	1.02 (0.394–1.66)
Terminal half-life$_{CNS}$, hours	499 (176)	477 (256–1010)
Distribution volume$_{CNS}$, L	1.65 (0.490)	1.58 (0.963–3.17)
Distribution volume$_{CSF}$, L	0.0314 (0.0183)	0.0272 (0.00629–0.0989)
Clearance$_{systemic}$, L/hour	3.04 (0.600)	2.80 (2.30–4.39)
Elimination half-life, hours	16.5 (5.72)	14.5 (8.83–30.6)
Distribution volume$_{systemic}$, L	73.7 (33.2)	71.5 (32.3–155)

CNS, central nervous system; CSF, cerebrospinal fluid.

serum (**Figure 4**). In addition, the fixed effect parameters were estimated with good precision, except for the proportionality coefficients for V_{CSF} and V_{CNS} (76.1% relative standard error (RSE) and 121% RSE, respectively) and the transit rate constant, K_{trans} (40.2% RSE; **Table 1**). This may be expected given that only trough concentrations in the CSF were available. The precision of the interindividual variability estimates was poor, as may be expected given the small sample size, and the residual variability estimates indicated a high degree of variability from other sources (**Table 1**). Shrinkage estimates were calculated as a measure of the tendency of the Bayesian individual parameter estimates to shrink toward the mean value.[21] These estimates were generally high for each of the interindividual variability random effects, with the exception of $V_{central}$, K_{trans}, and V_{CSF}; shrinkage in the residual variability random effects was low (**Table 1**).

The performance of the PK model was evaluated by performing a visual predictive check with 500 simulation replicates of the original dataset in dose and occasion subgroups (**Figure 5**). For both CSF and serum, the observed median TAK-611 concentrations

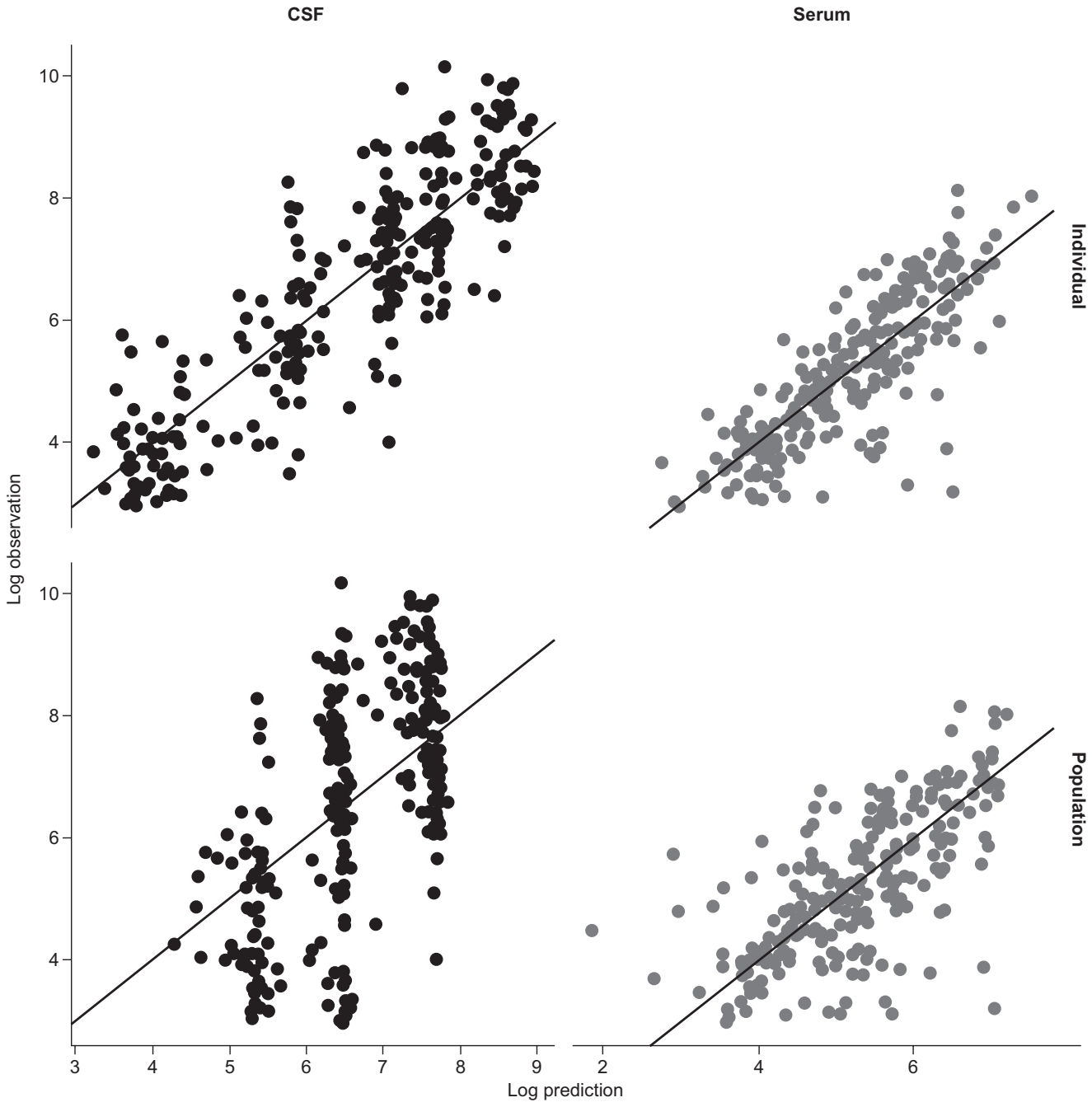

Figure 4 Observed versus predicted TAK-611 concentrations in CSF and serum. CSF, cerebrospinal fluid.

were within the 90% CI of the simulated median concentrations at most time points in all dose groups (**Figure 5a,b**), again suggesting that the data were well characterized by the PK model. Numerical predictive checks for serum and CSF are shown in **Table S1**.

Simulation results

The PK model was applied to simulate concentrations of TAK-611 in the CSF and CNS over time for different dose regimens, using a weekly PK sampling simulation for all regimens (**Figure S2**). At 100 mg EOW, the simulation predicted that it would take ~ 16 weeks to achieve steady-state, which is consistent with the dosing interval of 2 weeks and the median terminal half-life of distribution from the CNS brain tissue of 477 hours (2.8 weeks).

Higher trough concentrations were maintained when an initial weekly dosing regimen was simulated (weekly dosing for 12 weeks with TAK-611 100 or 150 mg, followed by dosing EOW) compared with the 100 mg EOW regimen (**Figure S2**). Consistent with the transition from weekly to EOW dosing, these simulations were associated with a predicted rapid accumulation of TAK-611 to a high concentration in both the CSF and CNS, followed by a fall toward the lower steady-state concentration. The

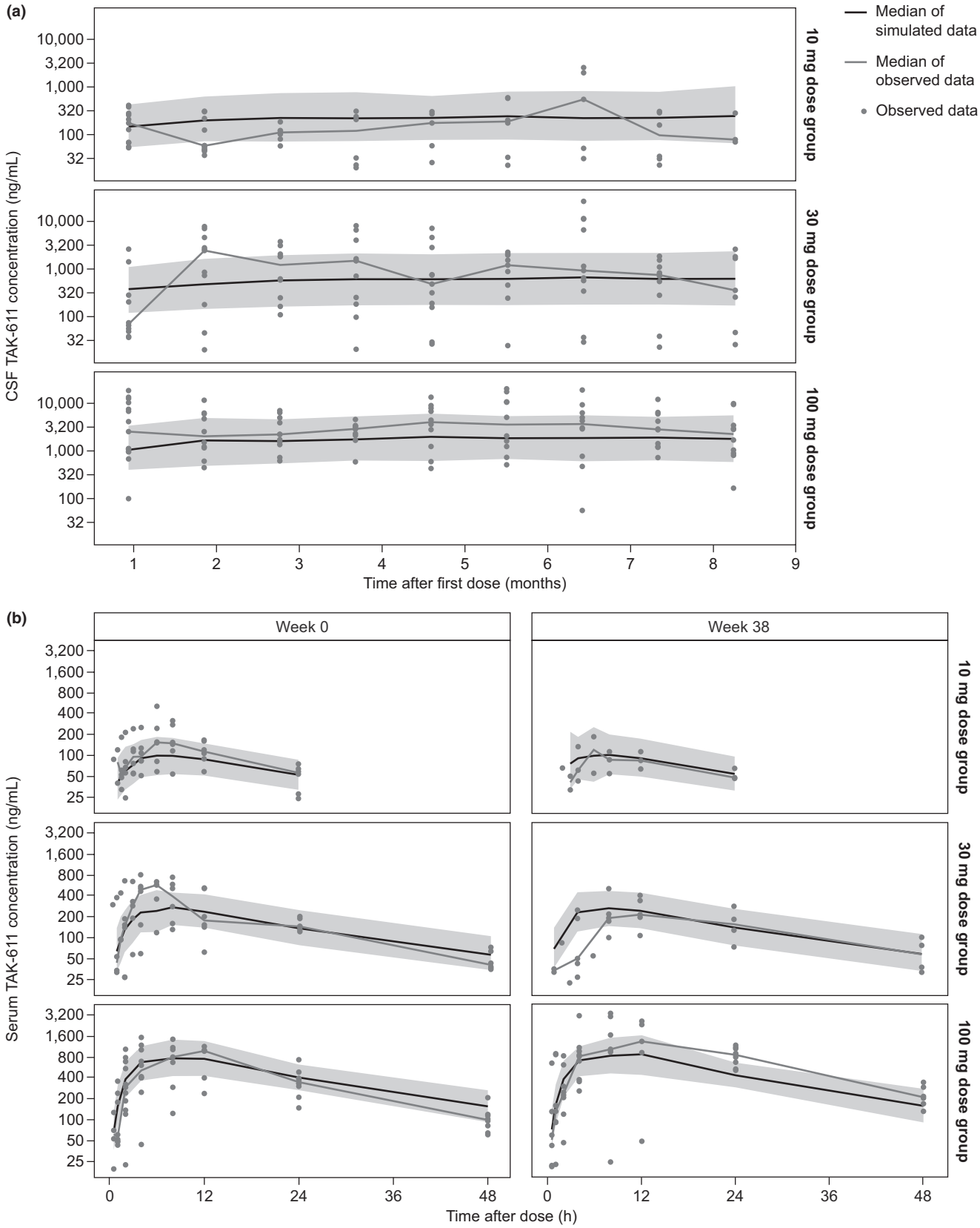

Figure 5 Visual predictive check of TAK-611 concentrations in (**a**) CSF and (**b**) serum. Gray shaded area indicates 90% confidence intervals of simulated medians. CSF, cerebrospinal fluid.

highest predicted steady-state TAK-611 concentrations overall were observed using a 150 mg weekly dosing simulation throughout the 2-year period, with concentrations approximately twice as high as those observed with the simulation of 150 mg initial weekly dosing followed by 150 mg EOW, in both the CSF and CNS. The simulations also suggested that use of an age-based dosing scenario, in which the dose was increased in line with age, would generally achieve more consistent steady-state trough concentrations of TAK-611 over time for all three age groups (data not shown).

DISCUSSION

The aim of this analysis was to develop a population PK model to describe the disposition of TAK-611 following IT administration in patients with MLD. We found that the sparse CSF concentration data and dense serum concentration data from the phase I/II trial of IT TAK-611 were well characterized by a model that included a putative CNS tissue compartment alongside central CSF and serum compartments. Evaluation of the model generally confirmed its ability to reproduce observed measurements effectively at the individual and population levels, supporting its further use. We anticipate that development of pharmacodynamic (PD) analyses based on this PK model is likely to be an important next step for evaluating and predicting treatment outcomes in patients receiving this investigational therapy.

Although our initial model was based on serum and CSF compartments only, we found that an additional compartment peripheral to the CSF was necessary to characterize the data. We inferred that this may represent a component of brain tissue in the CNS. Potential mechanisms by which TAK-611 could enter the brain parenchyma include transependymal movement from ventricles through ependymal cells via gap junctions,[22] and perivascular and paravascular (glymphatic) movement via the pia/glia limitans.[23–26] Inclusion of a transit compartment in the model was necessary to account for the delayed appearance of TAK-611 in serum, which is likely to reflect CSF drainage into the systemic circulation via the glymphatic and lymphatic systems.[27–29]

Body weight was used as a covariate to allometrically scale the systemic components of the model. Incorporation of predicted age-based CSF and CNS volumes[20] in place of body weight-based volumes improved the overall fit of the model. Brain size (white matter, gray matter, and CSF volumes) develops on a different timescale to body weight, with rapid development during the first years of life and stabilization by age 4–5 years.[20] The use of different scaling methods for the brain and systemic components of the model, therefore, accommodated for these different physical maturation rates of the brain and the rest of the body. In addition, the relationship between age and weight is often more complex in children with late-infantile MLD than in healthy children. Body weight in children with MLD can be substantially reduced for age, partly as a result of progressive paralysis and loss of muscle mass owing to limited use,[5,30] whereas the correlation between age and brain size is relatively preserved by comparison. The use of age and body weight to scale different components of the model may allow further model scaling to more accurately simulate exposures in patients younger than those in this trial.

The individual parameter estimates provided further insights into TAK-611 disposition. The median transit half-life of TAK-611 from CSF to serum (1.19 hours) is consistent with the physiological rate of CSF turnover of four to six times per day.[31] In addition, the long terminal half-life of TAK-611 in the putative CNS compartment (almost 3 weeks) suggests significant uptake into brain tissue with a slow release back to the CSF, which would allow the drug to persist in the brain between doses delivered EOW. This extended persistence is likely to be important for the intended target site of the drug within the lysosomes of brain white-matter cells.

The investigation of several covariates during model development gave important insights into variables that may affect IT TAK-611 disposition. The comparable PKs of TAK-611 produced using the original and revised manufacturing processes was consistent with findings from nonclinical comparability studies,[15] and supports the relevance of the PK model for patients receiving TAK-611 produced by either process A or process B. Incorporation of continuous subject weight as a covariate did not confer any improvement on the serum PK model, which is likely to reflect the relatively limited weight changes in the population during the 10-month study period.

Although ADA titers were not included formally as covariates in the model, the graphical evaluation did not suggest a clear dose response for the production or neutralizing ability of ADAs. For some subjects, however, there was an apparent association between high ADA titers and reduced serum and/or CSF TAK-611 concentrations, particularly in the 10 mg dose group. Further investigations will be required to assess possible implications for treatment efficacy, because the effects of ADAs on treatment outcomes vary for other LSDs.[32] Over 200 disease-causing mutations have been identified for MLD; among these, some lead to the production of a nonfunctional ASA protein, whereas others result in heavily reduced levels of ASA expression.[33] In the phase I/II clinical trial, genetic analysis suggested that patients with the 465+1G>A null mutation, which is predicted to result in negligible levels of endogenous ASA, may be more likely to produce ADAs than individuals with other mutation types. These findings require further validation, but are consistent with previously reported associations between severe gene deletions/rearrangements and an increased likelihood of ADA production for other protein-based therapies.[34–37]

Simulations of TAK-611 trough concentrations in the CSF and CNS suggested that PK steady-state is achieved after ~ 16 weeks of treatment with the 100 mg EOW regimen, consistent with the predicted median TAK-611 elimination half-life of 477 hours for the CNS. Although dosing scenarios higher than 100 mg EOW were not evaluated in the phase I/II clinical study, the higher trough concentrations of TAK-611 predicted when simulating the 150 mg weekly dose or initial weekly dosing for 12 weeks with 100 or 150 mg may support further investigation of these alternative regimens. The nonclinical studies of TAK-611 did not measure a steady-state trough concentration in the CSF, which could have been used to define a target concentration for these simulations. The observed clinical effects on decreased CSF sulfatides, motor function, and brain tissue changes will require further evaluation to identify a target clinical CSF concentration.

Although the data were generally well characterized by the PK model, it is important to consider the limitations of the approach. As may be expected for studies involving rare diseases, the study sample size was small, leading to a lack of precision, especially in interindividual variability estimates. In addition, missed doses and measurements for some subjects further reduced the amount of data available for model development. However, missed doses may also have helped to improve the estimates of TAK-611 terminal half-life in the CNS, by providing CSF concentrations that were measured > 2 weeks after the previous dose. The sparse sampling of CSF TAK-611 concentrations also presented a challenge during model development, and the description of the concentration profile and model parameter estimates could be improved by recording CSF TAK-611 levels at one or more additional time points. In addition, the inability to include ADA titer as a formal covariate during model development may have biased certain results; for example, efficacy predictions in future PK/PD modeling may be underestimated. The age-based scaling applied to the model may also have been further improved by using observed CNS and CSF volumes obtained via brain magnetic resonance imaging from the children in this study given that children with MLD tend to have slightly reduced gray matter volumes relative to healthy children.[38,39]

Despite these limitations, the PK model effectively characterizes the disposition of TAK-611 following IT delivery in patients with MLD. The rapid uptake (distribution) and the predicted long half-life of the drug in the CNS between doses support the use of IT administration as an effective method of delivering TAK-611 to the intended target site. In the future, this model will be used as the basis for development of PK/PD analyses to explore the relationship between drug concentration in the CSF and relevant functional outcomes for patients, including CSF sulfatide concentrations, brain tissue changes, and motor function outcomes as assessed by GMFM-88 total score.[16,17] Such analyses will provide important insights into the target TAK-611 exposure required to achieve therapeutic efficacy. Ultimately, this will help to guide decisions on the most appropriate dosing regimens and inform future development of this investigational therapy.

SUPPORTING INFORMATION

Supplementary information accompanies this paper on the *Clinical Pharmacology & Therapeutics* website (www.cpt-journal.com).

Figure S1. Influence of ADAs on TAK-611 concentration in (**a**) CSF and (**b**) serum at week 38.
Figure S2. Simulated median TAK-611 trough concentrations by dose regimen.
Table S1. Numerical predictive check of TAK-611 concentrations in CSF and serum.
Data S1. Model code.

ACKNOWLEDGMENTS

The authors thank all the patients and their families for their participation in the study.

FUNDING

This study was funded by Shire (a member of the Takeda group of companies). Metrum Research Group performed the data analysis, which was funded by Shire (a member of the Takeda group of companies). Medical writing support was provided by Dr. Jessica Hardy of Oxford PharmaGenesis, Oxford, UK, and was funded by Shire (a member of the Takeda group of companies).

CONFLICT OF INTEREST

Steven Troy was an employee of Shire (a member of the Takeda group of companies) at the time this research was performed, is a Takeda stock owner, and is now an employee of Radius Health. Margaret Wasilewski was an employee of Shire (a member of the Takeda group of companies) when this research was performed and is a Takeda stock owner. Jack Beusmans and C.J. Godfrey are employees of Metrum Research Group.

AUTHOR CONTRIBUTIONS

S.T., M.W., J.B., and C.J.G. wrote the manuscript. S.T. and M.W. designed the research. S.T., J.B., and C.J.G. performed the research. J.B. and C.J.G. analyzed the data.

DATA AVAILABILITY STATEMENT

Shire (a Takeda company) does not plan to share data supporting the results reported in this article.

1. Gieselmann, V. Metachromatic leukodystrophy: genetics, pathogenesis and therapeutic options. *Acta Paediatr.* **97**, 15–21 (2008).
2. von Figura, K., Gieselmann, V. & Jaeken, J. Metachromatic Leukodystrophy. In *Scriver's Online Metabolic and Molecular Bases of Inherited Disease* (eds. Valle, D. *et al.*) Chapter 148 (McGraw-Hill, New York, 2001).
3. van Rappard, D.F., Boelens, J.J. & Wolf, N.I. Metachromatic leukodystrophy: disease spectrum and approaches for treatment. *Best Pract. Res. Clin. Endocrinol. Metab.* **29**, 261–273 (2015).
4. Kehrer, C. *et al*. Language and cognition in children with metachromatic leukodystrophy: onset and natural course in a nationwide cohort. *Orphanet J. Rare Dis.* **9**, 18 (2014).
5. Gieselmann, V. & Krageloh-Mann, I. Metachromatic leukodystrophy - an update. *Neuropediatrics* **41**, 1–6 (2010).
6. Kehrer, C., Blumenstock, G., Gieselmann, V., Krageloh-Mann, I. & German, L. The natural course of gross motor deterioration in metachromatic leukodystrophy. *Dev. Med. Child Neurol.* **53**, 850–855 (2011).
7. Biffi, A., Lucchini, G., Rovelli, A. & Sessa, M. Metachromatic leukodystrophy: an overview of current and prospective treatments. *Bone Marrow Transplant.* **42** (suppl. 2), S2–S6 (2008).
8. Martin, H.R., Poe, M.D., Provenzale, J.M., Kurtzberg, J., Mendizabal, A. & Escolar, M.L. Neurodevelopmental outcomes of umbilical cord blood transplantation in metachromatic leukodystrophy. *Biol. Blood Marrow Transplant* **19**, 616–624 (2013).
9. Boucher, A.A. *et al*. Long-term outcomes after allogeneic hematopoietic stem cell transplantation for metachromatic leukodystrophy: the largest single-institution cohort report. *Orphanet J. Rare Dis.* **10**, 94 (2015).
10. Baldo, B.A. Enzymes approved for human therapy: indications, mechanisms and adverse effects. *BioDrugs* **29**, 31–55 (2015).
11. Muenzer, J. *et al*. Ten years of the Hunter Outcome Survey (HOS): insights, achievements, and lessons learned from a global patient registry. *Orphanet J. Rare Dis.* **12**, 82 (2017).
12. Felice, B.R. *et al*. Safety evaluation of chronic intrathecal administration of idursulfase-IT in cynomolgus monkeys. *Toxicol. Pathol.* **39**, 879–892 (2011).

13. Calias, P. *et al*. CNS penetration of intrathecal-lumbar idursulfase in the monkey, dog and mouse: implications for neurological outcomes of lysosomal storage disorder. *PLoS One* **7**, e30341 (2012).
14. Muenzer, J. *et al*. A phase I/II study of intrathecal idursulfase-IT in children with severe mucopolysaccharidosis II. *Genet. Med.* **18**, 73–81 (2016).
15. Wright, T. *et al*. Nonclinical comparability studies of recombinant human arylsulfatase A addressing manufacturing process changes. *PLoS One* **13**, e0195186 (2018).
16. Giugliani, R. *et al*. Safety and efficacy of intrathecal delivery of recombinant human arylsulfatase A in children with late-infantile metachromatic leukodystrophy. *Ann. Neurol.* **84**, S396 (2018).
17. Russell, D.J., Rosenbaum, P.L., Avery, L.M. & Lane, M. Gross Motor Function Measure (GMFM-66 and GMFM-88) User's Manual (Mac Keith Press, London, 2002).
18. Ahn, J.E., Karlsson, M.O., Dunne, A. & Ludden, T.M. Likelihood based approaches to handling data below the quantification limit using NONMEM VI. *J. Pharmacokinet. Pharmacodyn.* **35**, 401–421 (2008).
19. Yano, Y., Beal, S.L. & Sheiner, L.B. Evaluating pharmacokinetic/pharmacodynamic models using the posterior predictive check. *J. Pharmacokinet. Pharmacodyn.* **28**, 171–192 (2001).
20. Matsuzawa, J. *et al*. Age-related volumetric changes of brain gray and white matter in healthy infants and children. *Cereb. Cortex* **11**, 335–342 (2001).
21. Karlsson, M.O. & Savic, R.M. Diagnosing model diagnostics. *Clin. Pharmacol. Ther.* **82**, 17–20 (2007).
22. Casaca-Carreira, J., Temel, Y., Hescham, S.A. & Jahanshahi, A. Transependymal cerebrospinal fluid flow: opportunity for drug delivery? *Mol. Neurobiol.* **55**, 2780–2788 (2018).
23. Bacyinski, A., Xu, M., Wang, W. & Hu, J. The paravascular pathway for brain waste clearance: current understanding, significance and controversy. *Front. Neuroanat.* **11**, 101 (2017).
24. Bakker, E.N. *et al*. Lymphatic clearance of the brain: perivascular, paravascular and significance for neurodegenerative diseases. *Cell. Mol. Neurobiol.* **36**, 181–194 (2016).
25. Jolly, R.D., Marshall, N.R., Perrott, M.R., Dittmer, K.E., Hemsley, K.M. & Beard, H. Intracisternal enzyme replacement therapy in lysosomal storage diseases: routes of absorption into brain. *Neuropathol. Appl. Neurobiol.* **37**, 414–422 (2011).
26. Pizzo, M.E. *et al*. Intrathecal antibody distribution in the rat brain: surface diffusion, perivascular transport and osmotic enhancement of delivery. *J. Physiol.* **596**, 445–475 (2018).
27. Boulton, M., Flessner, M., Armstrong, D., Hay, J. & Johnston, M. Lymphatic drainage of the CNS: effects of lymphatic diversion/ligation on CSF protein transport to plasma. *Am. J. Physiol.* **272**, R1613–R1619 (1997).
28. Ma, Q., Ineichen, B.V., Detmar, M. & Proulx, S.T. Outflow of cerebrospinal fluid is predominantly through lymphatic vessels and is reduced in aged mice. *Nat. Commun.* **8**, 1434 (2017).
29. Iliff, J.J. *et al*. A paravascular pathway facilitates CSF flow through the brain parenchyma and the clearance of interstitial solutes, including amyloid beta. *Sci. Transl. Med.* **4**, 147ra111 (2012).
30. Eichler, F.S., Cox, T.M., Crombez, E., Dali, C.I. & Kohlschutter, A. Metachromatic leukodystrophy: an assessment of disease burden. *J. Child Neurol.* **31**, 1457–1463 (2016).
31. Sakka, L., Coll, G. & Chazal, J. Anatomy and physiology of cerebrospinal fluid. *Eur. Ann. Otorhinolaryngol. Head Neck Dis.* **128**, 309–316 (2011).
32. Harmatz, P. Enzyme replacement therapies and immunogenicity in lysosomal storage diseases: is there a pattern? *Clin. Ther.* **37**, 2130–2134 (2015).
33. Cesani, M. *et al*. Mutation update of ARSA and PSAP genes causing metachromatic leukodystrophy. *Hum. Mutat.* **37**, 16–27 (2016).
34. Linthorst, G.E., Hollak, C.E., Donker-Koopman, W.E., Strijland, A. & Aerts, J.M. Enzyme therapy for Fabry disease: neutralizing antibodies toward agalsidase alpha and beta. *Kidney Int.* **66**, 1589–1595 (2004).
35. Oldenburg, J. & Pavlova, A. Genetic risk factors for inhibitors to factors VIII and IX. *Haemophilia* **12** (suppl. 6), 15–22 (2006).
36. Pano, A., Barbier, A.J., Bielefeld, B., Whiteman, D.A. & Amato, D.A. Immunogenicity of idursulfase and clinical outcomes in very young patients (16 months to 7.5 years) with mucopolysaccharidosis II (Hunter syndrome). *Orphanet J. Rare Dis.* **10**, 50 (2015).
37. Wang, J. *et al*. Neutralizing antibodies to therapeutic enzymes: considerations for testing, prevention and treatment. *Nat. Biotechnol.* **26**, 901–908 (2008).
38. Groeschel, S. *et al*. Cerebral gray and white matter changes and clinical course in metachromatic leukodystrophy. *Neurology* **79**, 1662–1670 (2012).
39. Groeschel, S. *et al*. Effect of intrathecal recombinant human arylsulfatase A enzyme replacement therapy on structural brain MRI in children with metachromatic leukodystrophy. 13th European Paediatric Neurology Society (EPNS) Congress Abstract Book <http://www.epns2019.org/assets/EPNS_2019_ABSTRACT _BOOK_high_v2.pdf> (2019). Accessed January 17, 2020.